XIV CONGRESO GEOLÓGICO CHILENO
LA SERENA | OCTUBRE 2015

The dynamics of a tectonically controlled active silicic intrusion at Cordón Caulle volcano (Southern Andes) imaged by InSAR: building to the next eruption?

Francisco Delgado*, Matthew E. Pritchard
Department of Earth and Atmospheric Sciences, Cornell University, Ithaca, NY, USA

Fidel Costa
Earth Observatory of Singapore del Sur, SERNAGEOMIN, Temuco, Chile

Luis E. Lara, Daniel Basualto
Observatorio Volcanológico de los Andes del Sur, SERNAGEOMIN, Temuco, Chile

**Contact email: fjd49@cornell.edu*

Abstract. Cordón Caulle is a large fissural volcano which has erupted a continuous suite from basalts to rhyolites, including rhyolitic magma of the same composition in its past three historical eruptions in 1921, 1960 and 2011. There was siginificant ground deformation observed before and during the 2011-2012 eruption – here we use new InSAR results to document post-eruptive uplift of more than 0.75 m in in the past 3 years, likely produced by the same plumbing system that has been active during the historical eruptions.

Keywords: InSAR, volcano geodesy, Cordón Caulle volcano.

1 Introduction

Cordón Caulle is a volcanically active NW-SE elongated graben that is part of the larger Puyehue volcano – Cordillera Nevada chain that is thought to be tectononically controlled by a basement fault (Lara et al., 2006a). Even though the volcano is bimodal in composition, its most recent erupted products in the 1921, 1960 and 2011 eruptions are rhyodacites with the same chemical compositon (Singer et al., 2008; Castro et al., 2013), all with eruptive vents in either the S or N fissures that delimit the graben. Rhyolites are scarce in the Southern Andes and they have been proposed to be produced at Cordón Caulle by fractional crystalization from mantle derived basaltic melts with secondary crustal contamination and magma mixing, and enhanced by a local compressive stress regime (Singer et al., 20098; Lara et al., 2006a,b; Castro et al., 2013).

The 2011 eruption (VEI 4) was preceeded by a complex sequence of at least four years of ground uplift (Jay et al., 2014) and two months of seismic unrest (Cardona et al., 2012; Basualto et al., 2012). The eruption started in June 4th 2011 with the ejection of an eruptive column that reached elevations of ˜9-15 km (Lara et al., 2012). This first explosive stage ejected ˜0.25 km^3 of dense rock equivalent, lasted 27 hours and waned until June 15th when a rhyolitic flow was ejected from the same vent until March 2012, with a total volume of ˜0.45 km^3 (Bertin et al., 2012). Coeruptive subsidence of more than 1 m was observed at Cordillera Nevada caldera and Puyehue volcano during the three eruption days, and subsequent subsidence was located at the S part of the Cordón Caulle graben (Jay et al., 2014). The erupted products were stored at shallow reservoirs between 2-5 to 10 km infered from InSAR, Fe-Ti geobarometry (Jay et al., 2014) and experimental reproduction of the observed mineral phases in the erupted products (Castro et al., 2013). Altough the characteristic ground deformation pattern of dike intrusion was not clearly observed in multiple coeruptive interferograms (Jay et al., 2014), the presence of fracture swarms near the eruptive vents has been interpreted as being produced by a dike intrusion as the eruption triggering mechanism (Castro et al., 2013).

To seek a better understanding of the dynamics of the eruptive cycle and to understand the relation between magma storage, eruption and ground deformation at Cordón Caulle, we present new InSAR results spanning March 2012 to May 2015. Even tough the volcano enviromental conditions are not optimal for InSAR (e.g., Pinel et a., 2014; Dzurisin and Lu, 2007; Simons and Rosen, 2007; Lu and Dzurisin, 2014), hundreds of interferograms show that the volcano did not return to a state of calm after the eruption ended, as its surface has been uplifted since the end of eruption in March 2012 and is ongoing so far until May 2015. We note that this ground uplift has not been related to abnormal seismicity above background levels.

2 InSAR data processing

We use stripmap data acquired between 2012-2015 by the C band (5.6 cm wavelength) RADARSAT-2 (RS2) satellite, the X band (3.1 cm) COSMO-SkyMed (CSK) constellation of 4 satellites and the L band (23.6 cm) Uninhabited Aerial Vehicle Synthetic Aperture Radar (UAVSAR) airborne platform. Interferograms were

processed with the Caltech/Jet Propulsion Lab (JPL) InSAR Scientific Computing Environment (ISCE) software, and the UAVSAR data was processed by JPL and provided by the Alaska Satellite Facility (ASF). The RS2 (2012-2015) and UAVSAR data were acquired in a descending orbit while the CSK data was acquired in both descending (2012) and ascending (2013-2015) orbits. The topographic phase was removed with the 1 and 3 arcsec Shuttle Radar Topographic Mission (SRTM) digital elevation model for the RS2 and CSK datasets respectively. Due to the high temporal density and the availability of hundreds of CSK interferograms, we used the NSBAS time series method (López-Quiroz et al., 2009) as implemented in the GIANT toolbox (Agram et al., 2013) to retrieve the ground deformation time evolution. Time series mean velocities and single interferograms were downsampled (Lohman and Simons, 2005) and jointly inverted with the non linear neighbourhood algorithm (Sambridge, 1998) using standard formulas for the surface displacements produced by small pressuzired sphere (Mogi, 1958), a presurized elliposid (Yang, 1988) and a subhorizontal tensile dislocation (Okada, 1985) embedded in a linear elastic halfspace.

3 InSAR results

Due to rapid changes in the vegetation canopy surrounding the volcano, as well as the short wavelength of the RS2 and CSK radar signals, interferograms with temporal baselines longer than 1 month and 2 weeks are decorrelated outside of the volcano. Nevertheless, coherence is persistent at the less vegetated Cordón Caulle graben and Cordillera Nevada caldera for more than 1 year in the four data sets, and all of them show a persistent uplift signal between March 2012 and May 2015. The March-December 2012 CSK time series shows a maximum line of sight displacement of 40 cm in the central part of the Cordon Caulle graben, while the 2013-2015 CSK time series shows a maximum range change rate of ˜17 cm sightly shifted in horizontal location from the descending time series by the different line of the sight (Figures 1 and 2). The decomposition of the from ascending and descending line of sight range changes into EW and vertical displacements (Wright et al., 2004) and the use of an inverse model (next paragraph) predicts a maximum uplift rates of 45 cm/yr between March 2012 and December 2012 and 20 cm/yr between March 2013 and and May 2012. On the other hand, interferograms with short spatial and temporal baselines (1 day - 2 weeks) show lava flow subsidence with range change rates of ˜5-6 cm in 2 weeks.

The uplift signal is elongated and can not be explained a symmetrical source (Mogi, 1958), therefore we used two spherical source, a pressurized elliposid and a tensile dislocation. A presurized ellipoid predicts a large source at very shallow depths dimensions, while either two spherical sources or a subhorizontal tensile dislocation fit well the observed signal. The source depths are ˜4.5 and ˜6.5 km for the two spheres and the tensile dislocation with respect to the volcano mean base elevation. We prefer the tensile dislocation the sill source as it requires less bodies (Pascal et al., 2014). A more advanced distributed sill opening model can be calculated by expanding the sill dimensions in the strike and dip direction, and inverting for opening in small discretized patches. This model predicts maximum sill opening of ˜80 cm/yr between March 2013 and May 2015. On the other hand, the lava flow subsidence is interpreted as being produced by thermoelastic cooling and is significantly faster than InSAR detected subsidence at other volcanoes (Ebmeier et al., 2012).

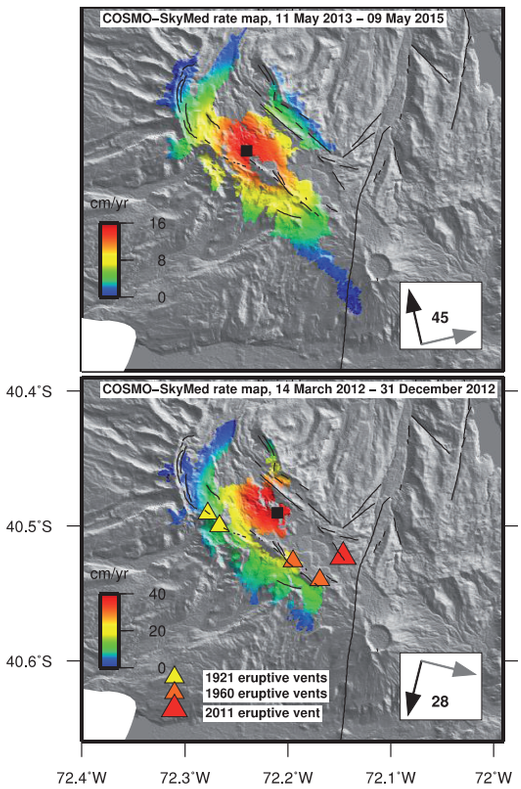

Figure 1. Cordón Caulle CSK mean line of sight velocities for the 2102 (left, descending) and 2013-2105 (right, ascending) periods draped over the SRTM topography. The black point shows the location of the time series shown in figure 2, the thin black lines are faults (Jay et al., 2014), the black arrow is the satellite heading, the grey arrow is the satellite line-of-sight (LOS) and the number in the white box is the satellite incidence angle. The shift in location of the black points and red areas of deformation are related to the change in LOS.

4 Discussion and conclusion

The inverted source depths are significantly deeper than those predicted for the volcano hydrothermal system (Sepúlveda et al., 2005), therefore we suggest that much of

the observed ground is of magmatic origin. We note that the shape and location of the signal is different that the ground pre eruptive uplift and co eruptive deflation (Jay et a., 2014) and that a change in the incidence angle due to the different ascending and descending orbits can not account for neither the shift in location or the signal elongation. As both the ground deformation signal and the modeled sill are elongated, we suggest that the sill is a tectonically controlled active intrusion (Lara et al., 2006b), altough the exact mechanism can not be solely deduced based on InSAR observations.

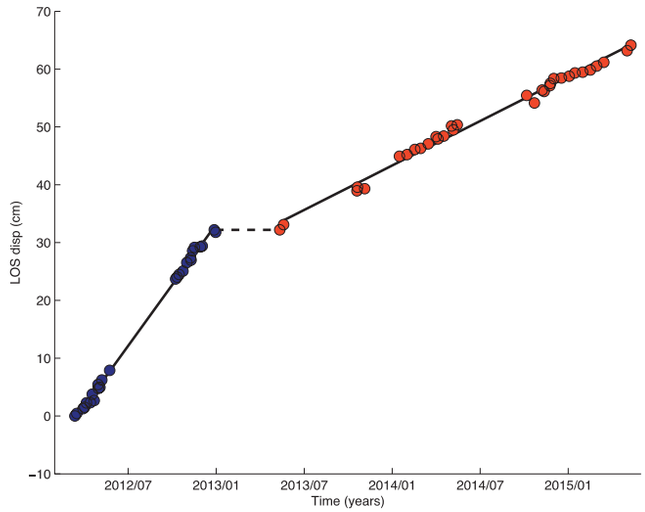

Figure 2. Line-of-Sight (LOS) displacements for the 2012 (blue) and 2013-2015 (orange) time series near the location of maximum observed deformation. The rate change in 2013 is partially explained by differences in the the line of sight for the ascending and descending interferograms.

We suggest that the ongoing ground uplift was triggered by the coeruptive pressure drop of a source beneath the Cordillera Nevada caldera that produced more than 1 m of ground subsidence (Jay et al., 2014). This can be explained by the Poiseuille flow law (Jaupart 2000; Lengliné et al., 2008; Pinel et al., 2010) which predicts that newtonian magma flow in vertical conduits is proportional to the pressure gradient which is largest after the end of an eruption due to the subsequent magma chamber deflation. Although the point of maximum uplift does not coincide with the location of the coeruptive source, the sill overlaps it.

We propose that magma is intruding the large mush zone responsible for the 1921, 1960 and 2011 eruptions. Basaltic magmas mixed with the likely crystal-rich mush beneath the volcano at least 200 years before the 2011 eruption, and therefore did not triggered it, but likely provided heat to melt the rhyodacitic chamber, therefore we suggest that a similar mechanism is responsible for the ongoing ground uplift (Jay et al., 2014). However, the exact mechanism of ground uplift, whether the uplift is produced by volatile exsolution or some other alternative mechanism can not be assessed based on geodetic data only and requires the use of other data sets such as chemistry of gas / water discharges or microgravity. Further work wil clarify the driving mechanism of the ongoing uplift.

Acknowledgements

This project is part of the CEOS Volcano pilot program coordinated by Mike Poland and Simona Zoffoli. We thank the space agencies for providing data (ASI, CSA, NASA, CNES). F.D. acknowledges CONICYT-Becas Chile for a Ph.D. grant.

References

Agram, P.S.; Jolivet, R.; Riel, B.; Lin, Y.N.; Simons, M.; Hetland, E.; Doin, M.P.; Lassere, C. 2013. New radar interferometric time series analysis toolbox released, Eos Trans. AGU, 94, 69.

Basualto, D.; Cardona, C.; Franco, L.; Gil, F.; Valderrama, A.; Hernández, E.; 2012. Mecanismos de intrusión relacionados con la erupción del complejo volcánico Cordón Caulle – Chile, Junio 4 de 2011. In Congreso Geológico Chileno, No. 13, Actas X: 522-524. Antofagasta.

Bertin, D.; Amigo, A.; Lara, L.E.; Orozco, G.; Silva, C. 2012. Erupción del Cordón Caulle 2011–2012: evolución de la fase efusiva. In Congreso Geológico Chileno, No. 13, Actas X: 539-541. Antofagasta.

Cardona, C.; Basualto, D.; Franco, L.; Gil, F.; Valderrama, A. Actividad sísmica relacionada con la erupción del Complejo Volcánico Cordón Caulle – Chile, Junio 4 de 2011. In Congreso Geológico Chileno, No. 13, Actas X: 536-538. Antofagasta.

Castro, J.M.; Schipper, C.I.; Mueller, S.P.; Militzer, a.S.; Amigo, A.; Parejas, C.S.; Jacob, D. 2013. Storage and eruption of near-liquidus rhyolite magma at Cordón Caulle, Chile. Bull. Volcanol. 75 (4), 702.

Dzurisin, D.; Lu, Z. 2006. Interferometric Synthetic Aperture Radar. In Volcano Deformation (Dzurisin, D. editor). Springer: 153–194. Berlin.

Ebmeier, S.K., Biggs, J., Mather, T.A., Elliott, J.R., Wadge, G., Amelung, F., 2012. Measuring large topographic change with InSAR: Lava thicknesses, extrusion rate and subsidence rate at Santiaguito volcano, Guatemala. Earth and Planetary Science Letters, 335-336, 216-225.

Jay, J.; Costa, F.,; Pritchard, M.; Lara, L.; Singer, B.; Herrin, J. 2014. Locating magma reservoirs using InSAR and petrology before and during the 2011–2012 Cordón Caulle silicic eruption. Earth and Planetary Science Letters, 395, 254-266.

Jaupart, C. 2000. Magma ascent at shallow levels. In Encyclopedia of Volcanoes (Sigurdsson, H., editor). Academic Press: 237-245. San Diego.

Lara, L.E.; Moreno, H.; Naranjo, J.a.; Matthews, S.; Pérez de Arce, C. 2006a. Magmatic evolution of the Puyehue–Cordón Caulle Volcanic Complex (40◦S), Southern Andean Volcanic Zone:

from shield to unusual rhyolitic fissure volcanism. J. Volcanol. Geotherm. Res. 157 (4), 343–366.

Lara, L.E.; Lavenu, A.; Cembrano, J.; Rodríguez, C. 2006b. Structural controls of volcanism in transversal chains: resheared faults and neotectonics in the Cordón Caulle–Puyehue area (40.5◦S), Southern Andes. J. Volcanol. Geotherm. Res. 158 (1–2), 70–86.

Lara, L.E.; Amigo, A.; Orozco, G.; Bertín, D. 2012. La erupción 2011-2012 del Cordón Caulle: antecedentes generales y rasgos notables de una erupción en curso. In Congreso Geológico Chileno, No. 13, Actas X: 525-527. Antofagasta.

Lengliné, O.; Marsan, D.; Got, J.-L.; Pinel, V.; Ferrazzini, V.; Okubo, P.G. 2008. Seismicity and deformation induced by magma accumulation at three basaltic volcanoes, J. Geophys. Res., 113, B12305.

Lohman, R.B.; Simons, M. 2005. Some thoughts on the use of InSAR data to constrain models of surface deformation: Noise structure and data downsampling. Geochem Geophys Geosyst, 6:Q01007.

López-Quiros, P.; Doin, M.-P.; Tupin, F.; Briole, P.; Nicolas, J.-M. 2009. Time series analysis of Mexico City subsidence constrained by radar interferometry. Journal of Applied Geophysics, 69, 1-15.

Lu, Z.; Dzurisin, D. 2014. InSAR Imaging of Aleutian Volcanoes. Springer: 383 p., Heidelberg.

Mogi, K. 1958. Relations between the eruptions of various volcanoes and the deformations of the ground surface around them. Bull Earthq Res Inst 36, 99-134.

Okada, Y. 1985. Surface deformation due to shear and tensile faults in a half-space. Bull Seismol Soc Amer, 75(4): 1135-1154.

Pascal, K., Neuberg, J., Rivalta, E., 2014. On precisely modelling surface deformation due to interacting magma chambers and dykes. Geophysical Journal International, 196, 253-278.

Pinel, V.; Jaupart, C.; Albino, F. 2010. On the relationship between cycles of eruptive activity and volcanic edifice growth. J. Volcanol. Geotherm. Res. 194(4):150–164.

Pinel, V.; Hooper, A.; Poland, M. 2014. Volcanology: Lessons learned from Synthetic Aperture Radar imagery, J. Volcanol. Geotherm. Res., 289, 81–113, doi: 10.1016/j.jvolgeores.2014.10.010.

Sambridge, M. 1999. Geophysical inversion with a neighbourhood algorithm—I. Searching a parameter space. Geophys J Int 138:479-494. doi:10.1046/j.1365-246X.1999.00876.x

Sepúlveda, F.; Dorsch, K.; Lahsen, A.; Bender, S.; Palacios, C. 2004. Chemical and isotopic composition of geothermal discharges from the Puyehue–Cordón Caulle area (40.5◦S), Southern Chile. Geothermics 33 (5), 655–673.

Simons, M.; Rosen, P. 2007 Interferometric synthetic aperture radar geodesy. In Treatise on Geophysics 3 (Herring, T.; editor. Elsevier Press: pp 391-446. Amsterdam.

Singer, B.S.; Jicha, B.R.; Harper, M.a.; Naranjo, J.a.; Lara, L.E.; Moreno-Roa, H. 2008. Eruptive history, geochronology, and magmatic evolution of the Puyehue–Cordón Caulle volcanic complex, Chile. Geol. Soc. Am. Bull. 120 (5–6), 599–618.

Wright, T.J.; Parsons, B.E.; Lu, Z. 2004, Toward mapping surface deformation in three dimensions using InSAR, Geophys. Res. Lett., 31, L01607.

Yang, X.; Davis, P.; Dieterich, J. 1988. Deformation from inflation of a dipping fi- nite prolate spheroid in an elastic half-space as a model for volcanic stressing. J. Geophys. Res. 93 (B5), 4249–4257.